

# Brain-controlled robot agent: an EEG-based e Robot agent

*Li-Wei Wu*

Department of Electrical and Control Engineering, National Chiao-Tung University, Hsinchu, Taiwan, Republic of China

*Hsien-Cheng Liao*

Information and Communications Research Laboratories, Industrial Technology Research Institute, Hsinchu, Taiwan, Republic of China, and

*Jwu-Sheng Hu and Pei-Chen Lo*

Department of Electrical and Control Engineering, National Chiao-Tung University, Hsinchu, Taiwan, Republic of China

### Abstract

**Purpose** – This paper aims to present a novel embedded-internet robot system based on an internet robot agent and the brain-computer interface (BCI) scheme.

**Design/methodology/approach** – A highly flexible and well-integrated embedded ethernet robot (e Robot) was designed with enhanced mobility. In the eRobot, a circuit core module called a tiny network bridge (TNB) is designed to reduce robotic system cost and increase its mobility and developmental flexibility. The TNB enables users to control eRobot motion via embedded ethernet technology. Through electroencephalogram (EEG) feedback training, the command translation unit (CTU) and alertness level detection unit (ADU) allow the eRobot to perform specific motions (for example, lying down or standing up) to reflect alertness levels of the user, and move forward, turn left or right following the user's command.

**Findings** – After a short training period, subjects could achieve at least 70 percent accuracy in the CTU game testing. And the error rate of ADU, estimated from the results of classifying 496 labeled EEG epochs, was approximately 10.7 percent. Combining an encoding procedure, the commands issued from the CTU could prevent the robot from performing undesired actions.

**Originality/value** – The e Robot could reflect some physiological human states and be controlled by users with our economical design and only two bipolar EEG channels adopted. Thus, users could make the EEG-based e Robot agent his or her representative. Based on the proposed EEG-based e Robot system, a robot with increased sophistication will be developed in the future for use by disabled patients.

**Keywords** Robotics, Man machine interface, Computer networks, Control systems

**Paper type** Research paper

## 1. Introduction

Since robots are developed, they are used in various applications and take on many different forms. Recently, a scheme called brain-computer interface (BCI), integrated of medicine and engineering, appears possible to provide a new choice for controlling a robot. Brain electrical activities recorded as multichannel electroencephalogram (EEG) signals have been used to investigate neurological disorders and brain function. Researchers have speculated that EEG signals could be used to control devices and the environment. The idea of a BCI was first introduced in 1973 (Vidal, 1973). In recent years, more than 40 research groups have attempted to develop an EEG-based BCI system by exploiting the

advantages of EEG – ease of recording and high temporal resolution. As has already been stated (Wolpaw *et al.*, 2000), a BCI is a communication system that does not depend on the brain's normal output pathways of peripheral nerves and muscles. In a BCI system, the EEG or event-related potential (ERP) of a subject is measured and sampled under a particular designed protocol (for example, by performing or imagining a movement of the left/right hand). Appropriate preprocessing, feature extraction and classification methods enable a BCI system to translate EEG signals into a series of commands.

Electrophysiological signals already used in BCI systems include slow cortical potentials (Karim *et al.*, 2006), visual evoked potentials (Middendorf *et al.*, 2000) and  $\mu$  or  $\beta$  rhythms (Pfurtscheller *et al.*, 2000, 2003; Pineda *et al.*, 2003; Wolpaw and McFarland, 2004). These signals are recorded from the scalp and then translated in real-time into commands for performing specific tasks. Pfurtscheller applied different motor imagery to BCI system control (Pfurtscheller *et al.*, 2000; Pfurtscheller and Neuper, 2001; Pfurtscheller *et al.*, 2003). Pfurtscheller focused mainly on the  $\mu$  rhythm (10–12 Hz) and the  $\beta$  band (14–20 Hz) at sites C3, Cz and C4, and achieved

---

The current issue and full text archive of this journal is available at [www.emeraldinsight.com/0143-991X.htm](http://www.emeraldinsight.com/0143-991X.htm)



Industrial Robot: An International Journal  
35/6 (2008) 507–519  
© Emerald Group Publishing Limited [ISSN 0143-991X]  
[DOI 10.1108/01439910810909501]

accuracy rates of over 80 percent (Pfurtscheller *et al.*, 2003). Additionally they designed a mechanical hand controlled by EEG activity recorded from a tetraplegic patient. After several months of training, the control accuracy rate was near 100 percent (Pfurtscheller and Neuper, 2001).

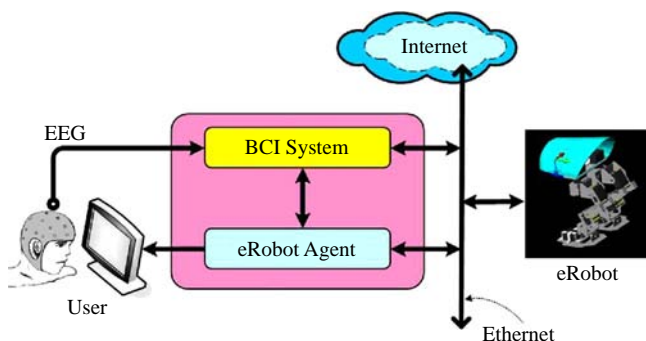
While BCI mechanisms have been extensively explored for online applications, there still exist limitations of low mobility. To deal with this issue, this work explored an innovative concept leading to a design for paralytic patients to efficiently interact with people and environment through a remote robot. We present an EEG-based eRobot agent designed by integrating advanced robot technologies with BCI mechanisms. The EEG-based eRobot agent based on embedded ethernet and BCI technology enables users to control a remote robot using their EEG signals. This remote-controlled eRobot is more flexible with better mobility, in comparison with those popular, well-developed BCI applications that mostly provide a communication channel between the environment and patients (e.g. the spellboard and cursor control applications; Kostov and Polak, 2000; Cheng *et al.*, 2001; Birch *et al.*, 2003; Pfurtscheller *et al.*, 2003; Wolpaw and McFarland, 2004; Karim *et al.*, 2006). Except translating EEG into commands to control the robot, this work also presents an alertness level detection system that identifies three states of mental alertness (alert, relaxation and sleep) in the BCI system. With its relatively economical design and only two bipolar EEG channels adopted, the eRobot can already reflect some physiological human states.

The rest of this paper is organized as follows. Section 2 briefly describes the EEG-based eRobot agent architecture. Section 3 then describes experiments in designing CTU. Next, Section 4 demonstrates the effectiveness of the proposed platform and presents the results of the BCI experiment. Conclusions are finally drawn in Section 5, along with recommendations for future research.

## 2. System architecture of the EEG-based eRobot agent

The system architecture of the EEG-based eRobot agent (Figure 1) comprises two parts – the embedded ethernet-based robot and the BCI system. The BCI system records a user's EEG signals and translates them into commands according to a user's intent and alertness level. The BCI system output is used to manage and control the embedded ethernet-based robot.

**Figure 1** Architecture of the EEG-based eRobot agent



### 2.1 BCI system

The BCI system consists of two major parts: the command translation unit (CTU), and the alertness level detection unit (ADU). The CTU extracts features from raw EEG signals and then categorizes the signals into requested types of motor imagery: imagination of right-hand or both-feet movement. The ADU primarily identifies subject level of alertness (alert, relaxation and sleep). Following a particular level of alertness, the eRobot may operate in a power-economical state or mimic human nature. Two channel EEG signals were acquired from the scalp, using a bipolar configuration – FC3-CP3 and FCz-CPz (Figure 2; Guger *et al.*, 2003).

#### 2.1.1 Command translation unit

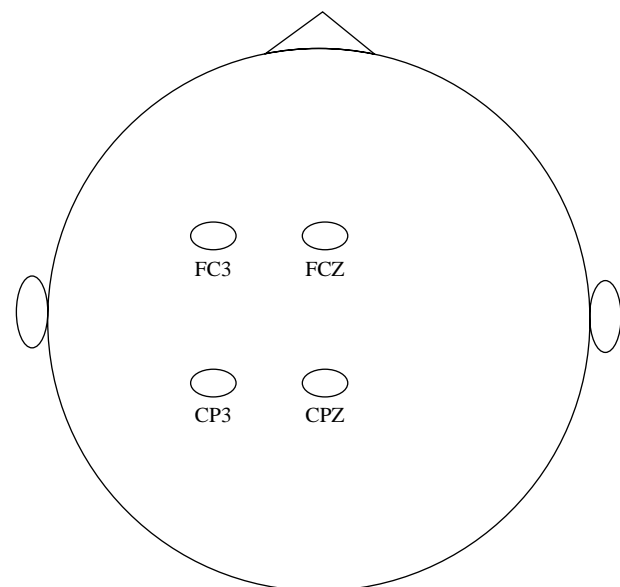
In this study, the band power scheme proposed in (Guger *et al.*, 2003) is used to design the CTU. However, a few modifications are made to feature quantification and categorization to improve the efficacy of the BCI-driven eRobot.

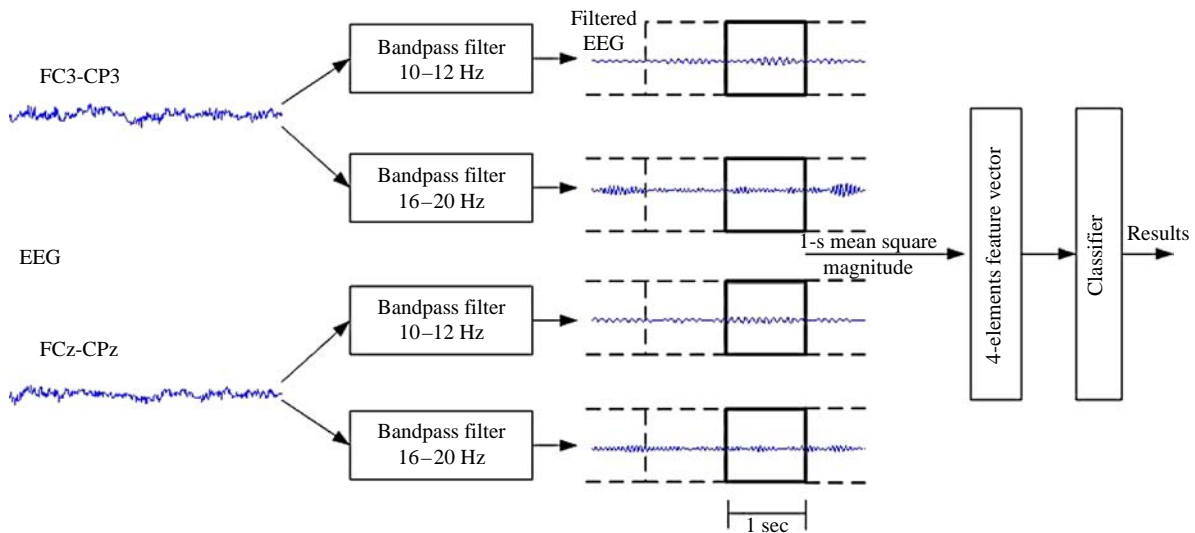
Users are instructed to imagine a right-hand movement or a both-feet movement to control the robot (Guger *et al.*, 2003). The EEG features are quantified by band power estimation. In each channel, the average  $\alpha$  ( $\beta$ ) power is estimated by computing the mean square magnitude of the frequency component within the range of 10–12 Hz (16–20 Hz), based on a one-second frame. Consequently, a four-feature vector is generated for each one-second frame, that is, average alpha power and average beta power at channels FC3-CP3 and FCz-CPz. As shown in Figure 3, the feature vector is then categorized by a subject-specific classifier developed by linear discriminant analysis (LDA). The LDA weighs each input parameter by its importance. The sign of the resulting sum of weighted parameters is used to determine the class of the input (Bishop, 1995). Experiments for determining weights of the classifier are drawn in Section 3.

#### 2.1.2 Alertness level detection unit (ADU)

The EEG  $\alpha$  rhythm, which commonly emerges during relaxation when eyes are closed, is suppressed by mental activities. In another aspect,  $\delta$  or  $\theta$  rhythms dominate during sleep

**Figure 2** Two bipolar channels recording montage



**Figure 3** Block diagram of feature quantifier in the CTU

(Ganong, 1991). Thus, the ADU employs these EEG characteristics for identifying three mental levels:

- 1 (alert) suppression of the  $\alpha$  rhythm;
- 2 (relaxation) increase of  $\alpha$  power; and
- 3 (sleep) emergence of  $\delta/\theta$  rhythms.

Figure 4 schematically presents a block diagram of the ADU. The subband-AR EEG classifier analyzes the EEG and determines whether the EEG epoch corresponds to one of the following patterns:  $\beta$  (14-20 Hz),  $\alpha$  (7-14 Hz) or  $\delta/\theta$  (0.5-7 Hz). According to classifier output, the alertness level determination determines the current alertness level (alert, relaxation, sleep) of the subject.

**2.1.2.1 Subband-AR EEG classifier.** The EEG signal is first decomposed into subband components using tree-structured filter banks (Figure 5). According to Gabor's uncertainty principle (Oppenheim *et al.*, 1998), downsampling enables the AR model to characterize the narrow-band, low-frequency EEG with enhanced accuracy (Liao and Lo, 2006). Accordingly, to improve frequency resolution and reduce computational load, a subband-filtering scheme is applied before the frequency analysis by AR model. A linear-phase lowpass FIR filter  $H(z)$  with a cutoff frequency of 30 Hz is employed as an anti-aliasing filter before downsampling. Then, the AR(2) model is applied to the decimated signal. Consider the EEG signal,  $x[n]$ , generated by an autoregressive (AR(2)) process that is driven by unit-variance white noise  $w[n]$ . An AR(2) model can be expressed as:

$$x[n] + a_2[1]x[n-1] + a_2[2]x[n-2] = w[n] \quad (1)$$

By solving the autocorrelation normal equations, model coefficients  $a_2[k]$ ,  $k=1,2$  can be determined and the conjugated pole pair is  $-(a_2[1]/2) \pm j(\sqrt{4a_2[2] - a_2^2[1]}/2)$ . The root frequency of  $output_1$  and  $output_2$  can be estimated from the phase of the pole. The phase (root frequency  $f_{r1}, f_{r2}$ ) can be derived as:

$$f_r = \sin^{-1} \left( \frac{\sqrt{(4a_2[2] - a_2^2[1])/4}}{\sqrt{a_2[2]}} \right) \quad (2)$$

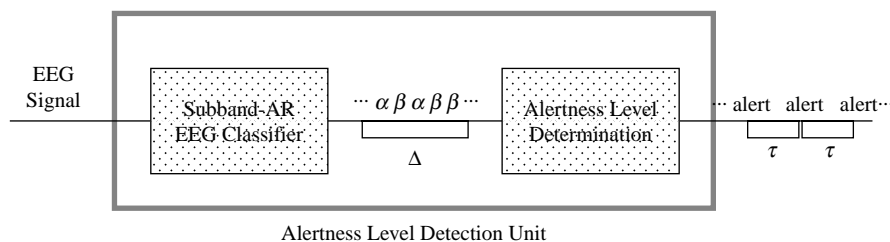
The magnitude of pole ( $|p_2|$ ) also can be derived. Notably,  $p_2$  denotes the AR(2)'s pole of  $output_2$  in Figure 5. The filtering-and-downsampling process is again repeated to maximize accuracy in discriminating between  $\alpha$  and  $\delta/\theta$  rhythms and the equivalent cutoff frequency is 15 Hz. Root frequency and magnitude are used to design an algorithm for classifying the EEG signal. The algorithm examines each windowed segment to check for the following criteria in order:

*Criterion -  $\delta/\theta$ :*  $f_{r,1} < 7$  Hz and  $f_{r,2} < 7$  Hz and  $|p_2| > 0.7$ ;

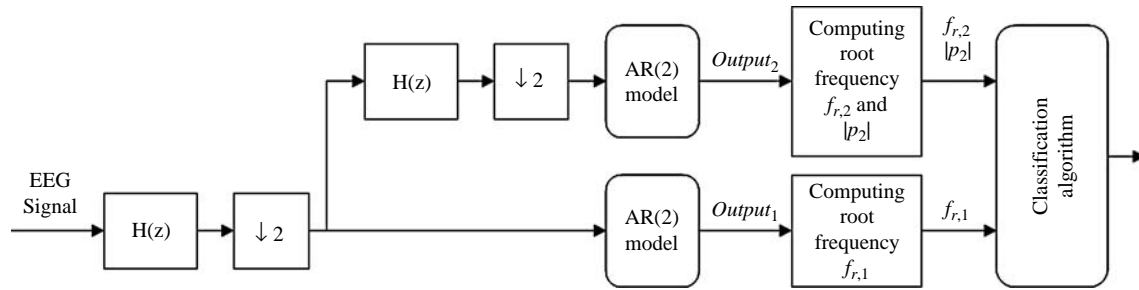
*Criterion -  $\alpha$ :*  $7$  Hz  $< f_{r,1} < 14$  Hz and  $7$  Hz  $< f_{r,2}$ ; (3)

*Criterion -  $\beta$ :*  $7$  Hz  $< f_{r,1}$  excluding segments recognized as  $\alpha$ .

The window length is 1 s, moving at a step of 0.5 s in this study. The criteria checkup is ordered according to characteristics of EEG. The  $\delta/\theta$  and  $\alpha$  rhythms are first recognized by their large amplitude and easily identifiable features. The root frequency

**Figure 4** Block diagram of the alertness level detection unit (ADU)

**Notes:** The subband-AR EEG classifier classifies the EEG as  $\alpha, \beta$  or  $\delta/\theta$  rhythms that are stored in a  $\Delta$  sec buffer. Then the alertness level determination updates the current alertness level of a user every  $\tau$  sec

**Figure 5** Tree-structured filter banks used to implement the subband-AR EEG classifier

$f_{r,1}$  is used to differentiate between the rhythmic band 0-7 Hz and 7-30 Hz band;  $f_{r,2}$  and  $|p_2|$  are used to identify the  $\delta/\theta$  rhythms. The length of  $p_2$  constrains signal amplitude and indicates the significance of the root frequency. The large amplitude of the  $\delta/\theta$  rhythm enables the constraints on  $|p_2|$  to be applied. The segments not satisfying any criterion in (3) are identified as  $\beta$  rhythms since, according to the hypothesis of the oscillatory model of the neuronal network, mental activity normally causes incoherent oscillation that results in amplitude cancellation (low power) and multi-frequency components (Klimesch, 1996).

The overall scheme is called a “subband-AR EEG classifier.” Notably,  $output_1$  and  $output_2$  are downsampling results (Figure 5), and the root frequency  $f_{r,i}$  should be further divided by  $2^i$ .

**2.1.2.2 Alertness level determination.** As mentioned in Section 2.1.2,  $\delta/\theta$ ,  $\alpha$  and  $\beta$  rhythms are employed to identify the mental states of sleep, relaxation and alert, respectively. A strategy that smoothly displays and tolerates errors is applied to improve ADU performance. A  $\Delta$ sec buffer ( $\Delta = 5$  herein) is created to store classification results (Figure 4). The current alertness level depends on the nearest 2s classification results. That is, the class that appears most often is regarded as the user’s current alertness level. The alertness level is updated every  $\tau$ s (herein,  $\tau = 1$ ). However, a blinking eye, which could be classified as a  $\delta/\theta$  rhythm, affects output. The sleep state must be further constrained to prevent misjudgment. The current alertness level is regarded as the sleep state unless the  $\delta/\theta$  rhythm exceeds 80 percent in the  $\Delta$ sec buffer. The buffer length was experimentally determined to improve performance of ADU.

## 2.2 Embedded ethernet-based robot (eRobot)

For combining with the BCI system adequately, an expression platform, called the embedded ethernet-based robot (eRobot), was designed. As stated in the Introduction, intelligent computing equipment can easily be integrated into the BCI system using ethernet. Design issues, electronic and mechanical systems of eRobot are described as follows.

### 2.2.1 Design issues of the eRobot system

The eRobot design is based on the characteristics of the BCI system. Two primary issues should be considered. First, since commands of present BCI systems could not be sophisticated enough and classification requires process time, a user cannot control the robot precisely. Hence, the robot should have autonomous motion control. Second, the proposed eRobot is considered a future home appliance application. Thus, it should be low cost, flexible, highly integrated, and small. Additionally, the communication

protocol must be sufficiently general, high speed and low cost, and the electrical design should be modularized so that users can extend more functions by adding different modules. The three-layer concept and implementation of the eRobot system are presented in the following sections.

### 2.2.2 The three layers concept of the eRobot system

The eRobot electronic system uses a general TCP/UDP/IP network and a combination of:

- 1 control and sensing layer (CSL);
- 2 gateway layer (GL); and
- 3 internet layer (IL).

The proposed three layers are as follows (Figure 6).

## 2.3 Control and sensing layer

The CSL manages motors control signals and sensor feedback (Figure 6). According to time trigger protocol, this layer can access each sensor datum and motor behavior. This layer is used by the robot to collect and dispatch environmental data.

## 2.4 Gateway layer

The GL manages the CSL data and provides low-level real-time control abilities, such as motion control, digital signal processing of sensor data, robot balance control, and embedded TCP/UDP/IP network packet translating. This layer also manages and determines which signals should be dispatched up a layer (IL) or processed in the GL. Some data types, such as that for streaming robot vision, are dispatched to the IL. Function of the GL is similar to the human spinal cord, facilitating robot reflex actions in real-time. In this manner, the GL reduces the computation effort of the robot agent and works effectively.

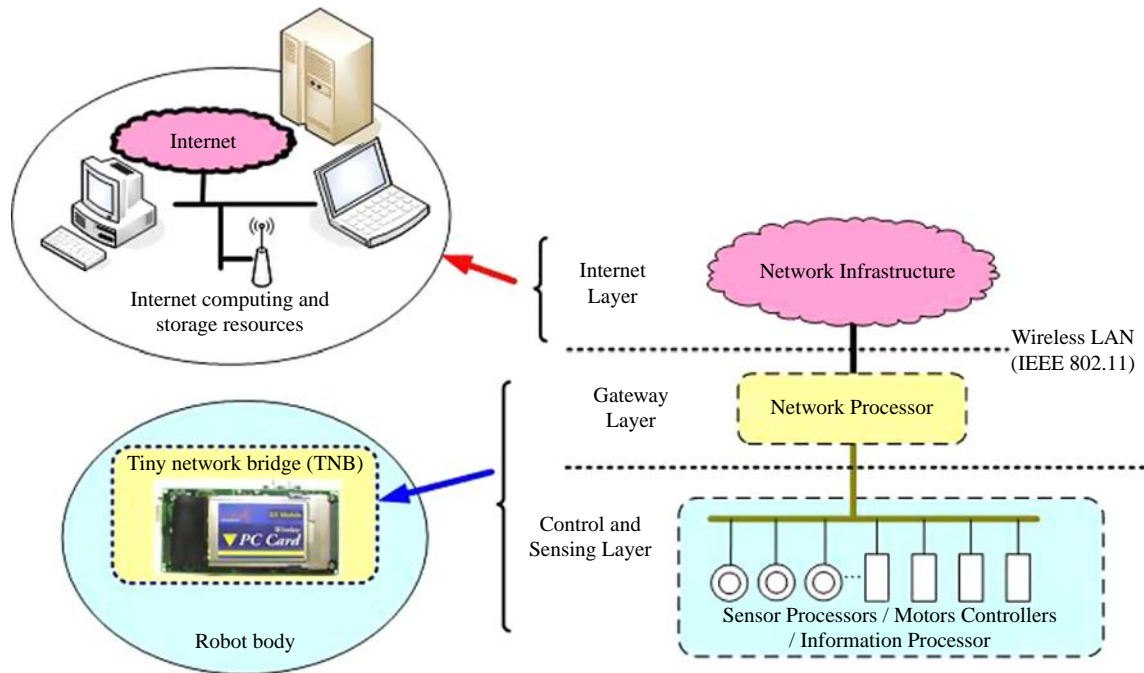
## 2.5 Internet layer

By utilizing TCP/UDP/IP integration, the robot can be connected to numerous computing resources, such as personal computers, PDAs and supercomputers. The robot can access infinite storage space and calculation resources. With a wide area network, the BCI system, which is regarded as the IL, can be used in distant locations.

The three-layer concept has been extensively applied in theses (Smith, 1998) and (Wu and Hu, 2005) works. In the eRobot system, the GL and CSL are realized as a hardware module (tiny network bridge, TNB) embedded with ethernet technology, and comprise a low-cost, highly integrated distributed architecture in a high speed and flexible ethernet environment for small robotic systems (Wu and Hu, 2004; Wu and Hu, 2005). Thus, the three-layer concept could



**Figure 6** The proposed design of the system employs an embedded TCP/UDP/IP network and the three layers concept



overcome design issues of the eRobot system described in Section 2.2.1.

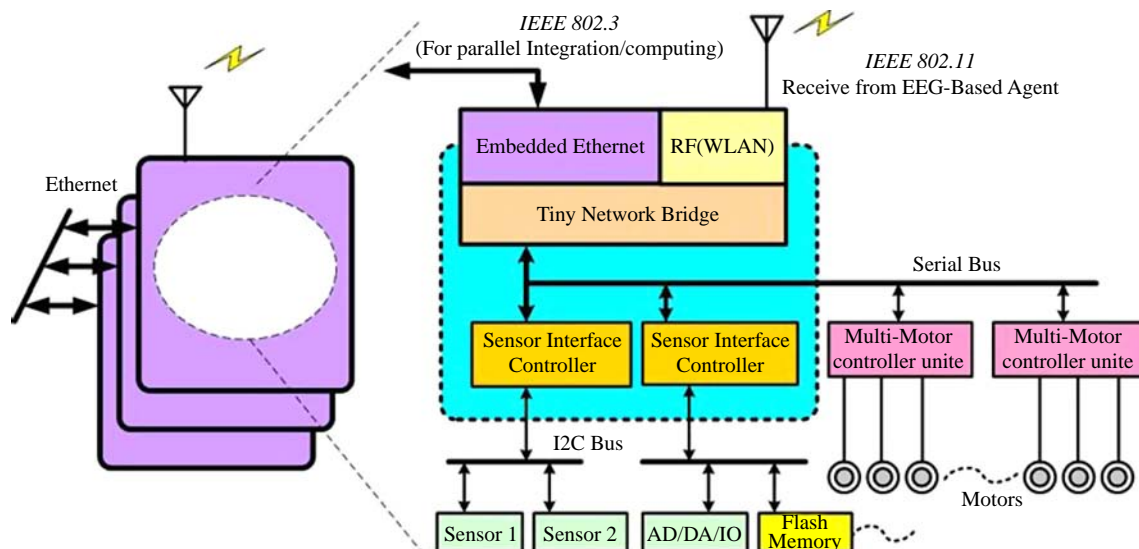
#### 2.5.1 Electronic and mechanical systems

Figure 7 shows the electronic architecture of eRobot. The primary electronic parts of eRobot are the TNB, multi-motor controller (MMC) units and sensor interface controller (SIC) units. The TNB, which consists of an 8-bit MCU (PIC-18F452), is based mainly on sensor network protocol (I<sub>2</sub>C bus) and a serial motion control network. The TNB coordinates eRobot actions and behaviors. Each MMC unit consists of an 8-bit MCU (PIC-16F877) that controls 16 motors (Futaba S-9402). The SIC unit is an 8-bit MCU

(PIC-18F452) device with an 8-channel analog-to-digital converter (ADC) and numerous digital interfaces, such as pulse width modulation and the I<sub>2</sub>C EEPROM file system (Bentham, 2002). By using the SIC units and time trigger protocol, the robot can detect in real-time information about its environment, including temperature, potential collision hazards, GYRO data, and acceleration values (Wu and Hu, 2004).

An elaborate TNB was designed to reduce robot system cost, increase its mobility, and flexibility during development. It provides a wireless LAN interface, allowing for easy implementation of the platform concept and integration using TCP/UDP/IP protocol. The IEEE802.11b and IEEE802.3

**Figure 7** e Robot electronic architecture



dual-mode network structures are adopted. The local area network interface uses the RTL8019 Chipset (10 Mbps) to access the IEEE802.3 network. Figure 8 presents a photograph of the TNB. The IEEE802.3 network provides many TNBs for parallel computing, linked according to TCP/UDP/IP protocol (Wu and Hu, 2004). Table I presents the TNB sensors.

After the user's EEG has been translated into commands and the alertness level has been determined, eRobot receives a motion command packet from the eRobot agent. The eRobot agent has a predefined motion command database from which a user selects a motion. The foregoing Figure 6 presents the principle interconnections structures involved in robot control. The motor systems are roughly arranged in a hierarchy. The upper levels (IL or GL) of the hierarchy send modulatory commands to lower levels (CSL), which in turn send back processed sensory and state information.

Figure 9 presents the mechanical design of the eRobot. This biped robot has 12 degrees of freedom. Actuators of eRobot consist of 12 sets of motors, gears, drivers and controllers. To achieve speed control, a quasi speed control system was developed by utilizing the direct kinematics of eRobot and Jacobian matrices that denote velocity relationships between joint angles, positions and the posture of each foot with respect to a robot coordinate frame fixed to the eRobot body. The eRobot forward kinematics, backward kinematics and balance of eRobot are controlled in coordinated motions, to move the eRobot forward or backward, to cause it to turn, walk, bend and stand up. Furthermore, walking and stable posture control approaches are described in (Hwang *et al.*, 2005).

The eRobot agent is set up at a remote station, so weight of robot can be reduced, thereby reducing robot power requirements. A motion integration program allows for prerecording and editing of robot behavior, and integration

of various sensors. This set-up facilitates use of other robot types for special applications.

### 3. Experiments

#### 3.1 Command translation unit

Currently, implementation of the CTU has two phases: training and controlling (Figure 10). During the training phase, the classifier is trained off-line to maximize the accuracy of classification results. During the controlling phase, the subject-specific linear classifier is used to translate the EEG signals into commands in a real-time manner.

The training phase is based mainly on Pfurtscheller's experimental paradigm (Guger *et al.*, 2001). The training phase for each subject comprised 5 sessions over 3 days. Each session was divided into 4 experimental runs, each run with 40 trials. Two types of training, training with and without biofeedback, were employed alternately to derive weight vectors of classifier to be used later in the controlling phase. The present design of the CTU requires it to make only two distinct motions controlled by two identifiable commands that are translated from two EEG features. Each subject was thus asked to perform two tasks: imagining either moving his or her right hand or moving both feet (Guger *et al.*, 2003). We used a stimulation unit, g.STIMunit (Guger Technologies OEG, Graz, Austria), to control the experimental paradigm. A real-time processing system, g.RTsys (Guger Technologies OEG, Graz, Austria), was applied to the data acquisition and EEG classification. The subject sat in a comfortable chair in front of a computer screen. In the beginning, a cross (+) was displayed in the screen center. At the 2nd second, a beep was sounded to draw the subject's attention. At the 3rd second, an arrow (cue stimulus) pointing to the right (or left) appeared for 1.25 s instructing the subject to imagine moving his or her

Figure 8 Photograph of the tiny network bridge module

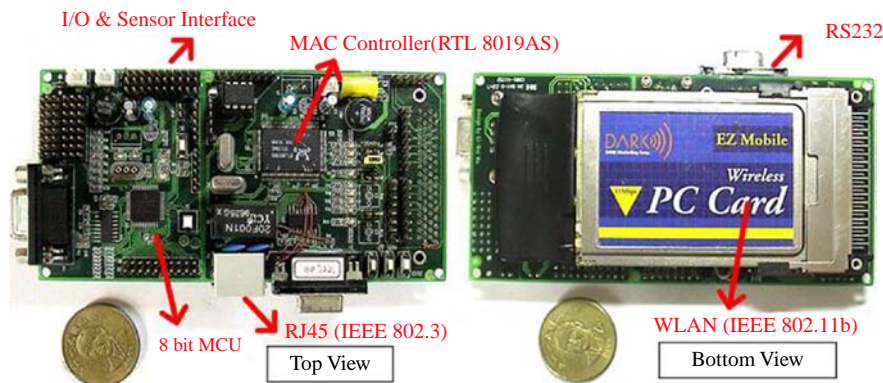
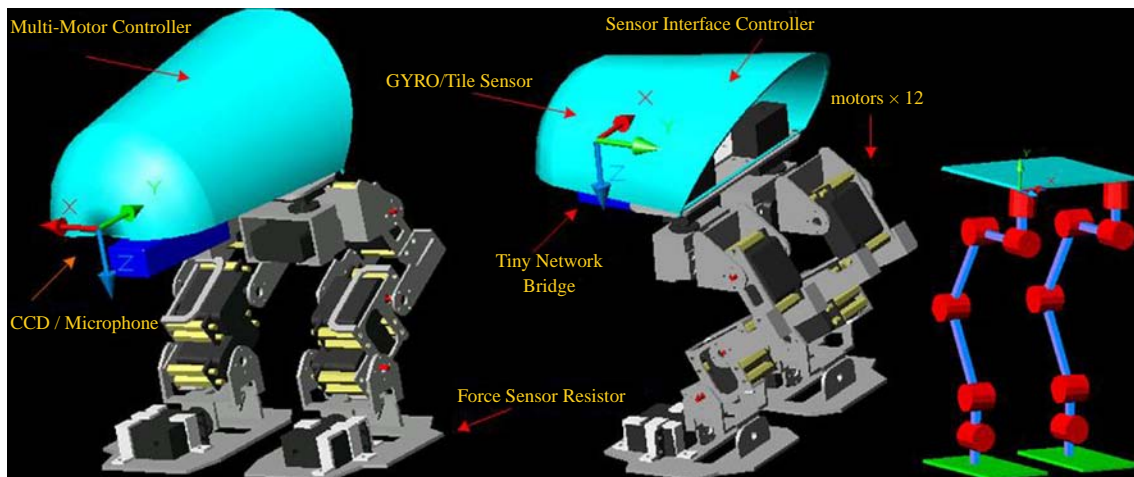
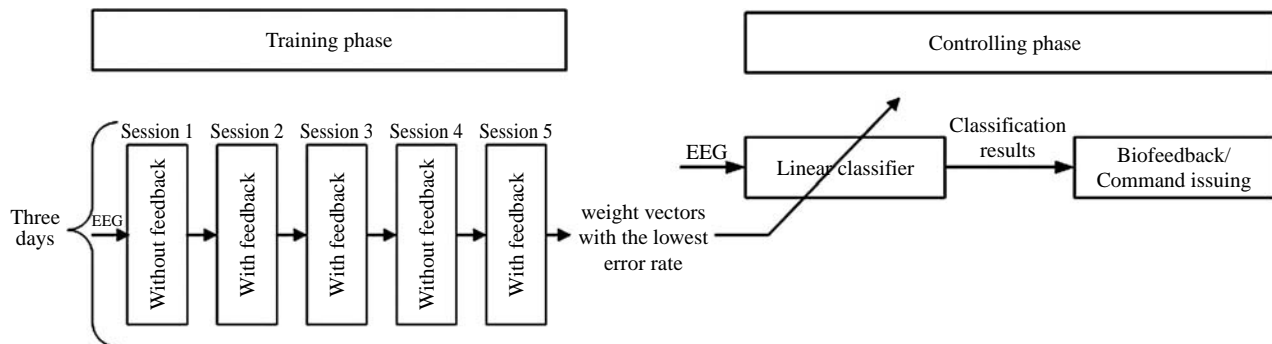


Table I Integrated sensors

Sensor	Type	Number
Tilt sensor (2-axis)	CXTA02 (Crossbow Technology, Inc.)	1
GYRO sensor	CRS 03-02 (Silicon Sensing Systems, Inc.)	1
Accelerometer (3-Axis)	CXL02LF3 (Crossbow Technology, Inc.)	1
Force sensing resistor	FS-101 (FlexiForce, Inc.)	6
Temperature/humidity sensor	SHT11 (Sensirion, Inc.)	1
Wireless vision module	OV18PW (ChinTAHO Technology, Inc.)	2

**Figure 9** e Robot mechanical design and 12 degrees of freedom**Figure 10** The two phases in CTU design

right hand or both feet until the trial ended. Each trial lasted 8 s. The EEG signals were digitized at a rate of 128 Hz.

About 160 trials were collected in one session. Each single trial contained an 8 s EEG, from which a four-feature vector was generated on a per-second basis. Accordingly, eight feature vectors were generated for each single trial. In the validation process, the data sets were randomly mixed and divided into ten partitions of equal size (that is, each partition contained 16 trials). To find the particular second (within the 8 s duration) with the lowest classification error, we conducted a ten times ten-fold cross validation: each partition was used in turn as the testing set to testify the error rate of the linear classifier trained by the remaining nine partitions. This resulted in ten error-rate sequences, which were averaged. This is the error rate of a ten-fold cross validation. To further improve the estimate the ten-fold cross validation is repeated ten times and all error rates are again averaged. Figure 11 presents the time courses for the error rates in one session. The weight vector of the classification time points with the lowest error rate (in the example, the Second 4) was employed during the feedback session in the training phase or later in the controlling phase.

During the feedback training, the EEG was classified online and the classification result was converted into a feedback stimulus – a horizontal bar displayed in the center of the monitor (Figure 12(a)). The bar varied in length according to

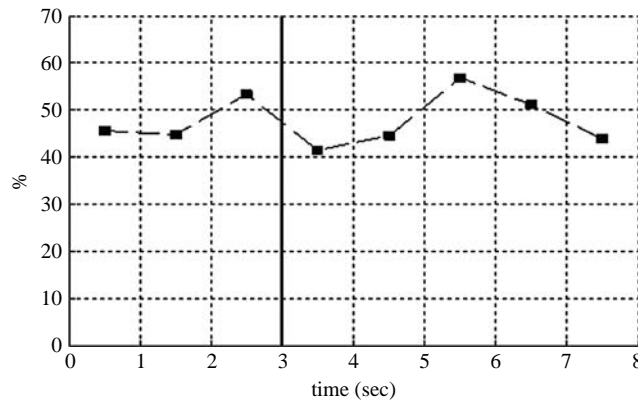
the output of classifier, which used the weights calculated from LDA to classify the feature vectors (Guger *et al.*, 2001).

During the controlling phase, classifier output was accumulated and shown on the monitor (Figure 12(b)). When accumulated output exceeded a predefined threshold, one command was issued. Then, the CTU switched to an inhibition period (1 s herein), during which no action was undertaken (Figure 12(c)). The scheme presented in Figure 12(b) was designed to extend the horizontal bar leftward or rightward as the subject imagined moving both feet (F) or the right hand (H).

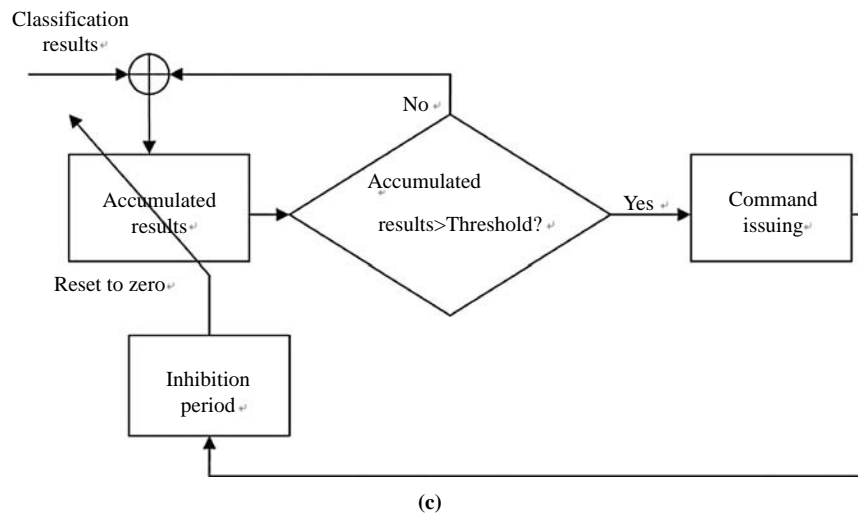
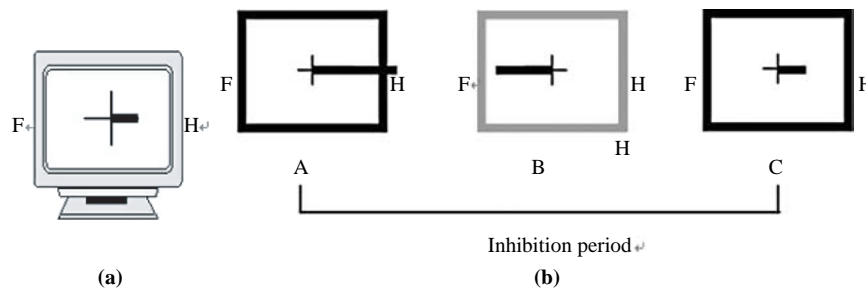
A simple game was designed to test the performance of the proposed CTU. In the game, a yellow target randomly appeared on the left or right side of the computer screen (Figure 13). Subjects were asked to imagine moving their right hand (both feet) when a right (left) target appeared. The purpose of imagined movement was to generate EEG patterns, to yield sufficient accumulated output to exceed the threshold, meaning that the target was reached. The subject earned 1 point when the target was hit; the target then disappeared.

### 3.2 Alertness level detection unit

The subject was asked to sit in a comfortable chair in front of a computer with a bio-feedback function. Ten-minute EEG was collected and used for offline classification. The EEG at channel FCz-CPz was examined to determine the ongoing

**Figure 11** Average error-rate sequence for one session containing 160 trials

**Note:** The vertical line indicates the time when the cue stimulus is applied (i.e., an arrow appears on the screen)

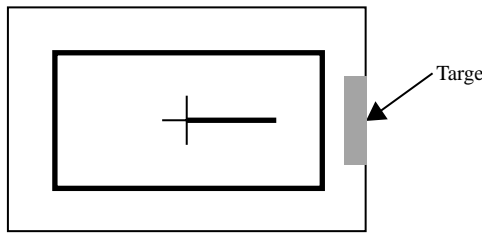
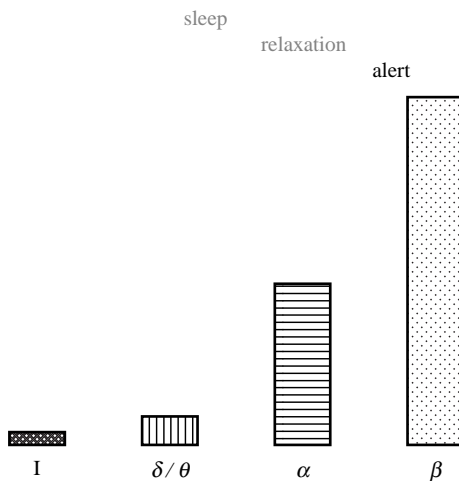
**Figure 12** (a) Biofeedback display during the training phase; (b) biofeedback display during the controlling phase

**Notes:** The bar length represents the accumulated output from the classifier. After the accumulated value exceeds a threshold (the left/right borderline), a command is issued (A) and the CTU switches to an inhibition period (B). Following the inhibition period (1 sec), the CTU again takes command (C). (c) Operation according to biofeedback scheme (controlling phase)

alertness level because the frontal lobes have been found to be involved in such higher cognitive functions like motor function, judgment, memory, social behavior, problem solving, etc. Output was transmitted to the eRobot Agent via ethernet. The display on the feedback computer was

divided into two parts. The heights of bars reflected the percentages of the three EEG patterns within a 2-second frame. The alertness level determination (ALD) based on classification results in the buffer yielded the current alertness level, which was displayed above the bars (Figure 14).



**Figure 13** Game for testing CTU performance**Figure 14** Display on the feedback computer

**Notes:** Bar heights reflected the percentages for the three EEG patterns within a 2-second frame. The bar "I" represents initiation

## 4. Results

The LDA and the Subband-AR EEG Classifier were implemented under Simulink (MathWorks, Inc., Natick, MA, USA) with Real-Time Workshop on a Pentium-M 1.4 (GHz) notebook. Real-Time Workshop can generate real-time code for operating in a real-time manner under Windows (Guger *et al.*, 2001).

### 4.1 Command translation unit

#### 4.1.1 Offline classification

The weights of the classification time points associated with the lowest classification error are then used to set up the classifier for each subject (Figure 10). Three healthy male volunteers at the mean age of  $26 \pm 3.8$  years participated in this experiment. The lowest classification error rates obtained by the three subjects were 22 percent, 38 percent, and 34 percent during the training phase (Table II). No subject had any experience with BCI before this experiment. The error rates were collected over five sessions, each consisting of 160 trials.

#### 4.1.2 A game testing

The subject had ten targets to be reached each round (Figure 13). All three subjects could achieve at least 70 percent accuracy after a short training period. Table III

**Table II** Error-rate sequences (in percentages) for three subjects are listed in (a)-(c). Results for five sessions are evaluated for each subject. The italicized numbers are the lowest error rates within a session

Session	1st s	2nd s	3rd s	4th s	5th s	6th s	7th s	8th s
<b>(a) Subject 1</b>								
1	50	46	47	50	35	31	38	45
2	46	52	48	49	36	24	22	29
3	42	49	49	55	37	30	33	31
4	52	48	44	46	43	34	30	34
5	51	47	50	53	32	33	42	34
<b>(b) Subject 2</b>								
1	49	54	49	42	41	55	50	50
2	64	49	48	42	47	47	50	46
3	49	51	52	40	48	55	45	42
4	52	46	44	42	45	51	50	50
5	54	53	56	49	49	38	44	54
<b>(c) Subject 3</b>								
1	41	49	55	54	60	49	39	56
2	53	54	48	44	34	50	52	49
3	54	47	38	35	46	47	43	36
4	45	46	55	55	49	54	40	48
5	45	44	42	44	40	49	40	51

**Table III** Results of game testing

	Time required per round (s)	Mean time per command (s)
Subject 1	105	10.5
Subject 2	129	12.9
Subject 3	118	11.8

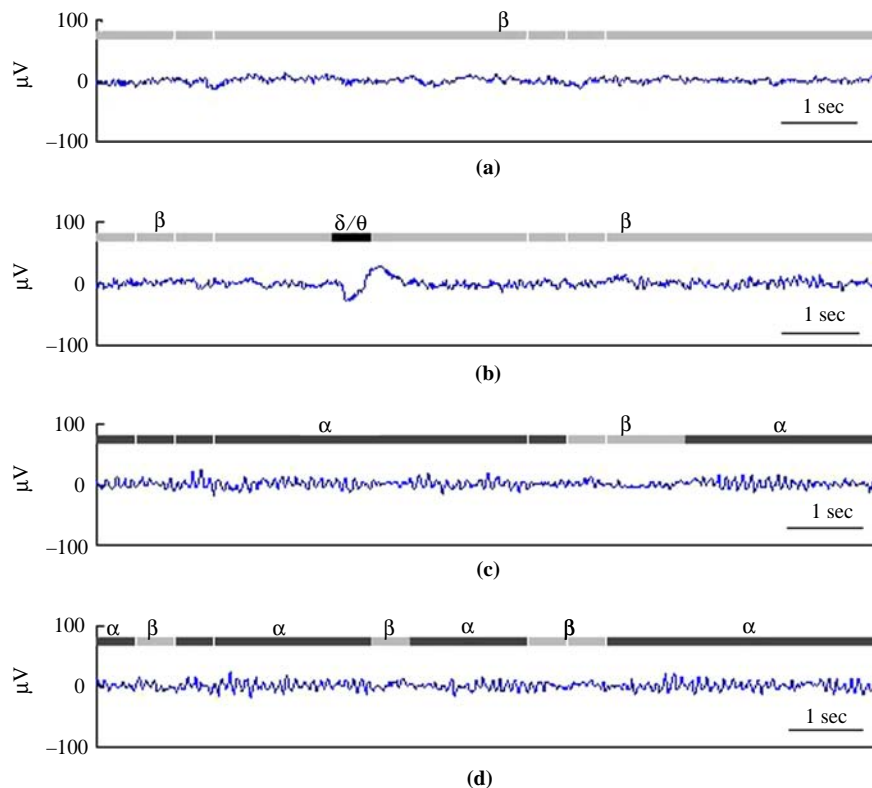
lists the average time required by each subject to issue a command under an accuracy rate of 70 percent.

### 4.2 Alertness level detection unit

Figure 15 presents a part of our classification results. Empirical EEG data were firstly labeled by an experienced EEG expert based on naked-eye examination. Results of interpretation conclude 184  $\delta/\theta$ s, 131  $\alpha$ s, and 181  $\beta$ s. The error rate, estimated from the results of classifying 496 labeled EEG epochs, was approximately 10.7 percent. Table IV is the confusion matrix. Each row represents the classification result for each class. According to the table,  $\beta$  activities tended to be classified as  $\delta/\theta$  activities, which might be due to the EOG interference.

### 4.3 Overall system

Figure 16 presents the combination of the CTU and the ADU. The sequence of the issuing commands from the CTU is encoded to prevent the robot from performing undesired actions. For instance, a user may generate four consecutive L commands (L/R represent the horizontal bar extending leftward/rightward), representing the action "turn left" (shown on the top of the right-hand column in Figure 16). According to game testing results, the probability of making

**Figure 15** Classification results for real EEG signals**Table IV** The confusion matrix

	$\delta/\theta$	$\alpha$	$\beta$
$\delta/\theta$	177	2	5
$\alpha$	5	122	4
$\beta$	27	10	144

a false action “turn right” (desired action is “turn left”) is around 0.0081 ( $0.3 \times 0.3 \times 0.3 \times 0.3$ ). Figure 17 presents the overall system after the CTU and ADU have been applied. A user can control the remote robot in real-time, and the user’s alertness level can be represented using a pre-defined motion.

## 5. Conclusion and discussion

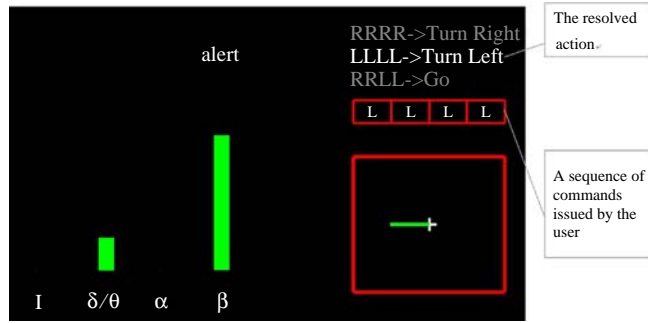
This work presents a novel embedded ethernet robot system, which is controlled by human EEG signals. This preliminary study focuses on implementing the entire system and the BCI schemes integrated with alertness level detection to improve robot performance. As the accuracy of the CTU is not very high, care must be taken to avoid false actions. Hence, the encoding process is adopted to determine robot action. The TNB and only two bipolar EEG channels were adopted to decrease the cost of the robotic system and increase its mobility and developmental flexibility. Based on the proposed EEG-based eRobot system, a robot with increased sophistication will be developed in the future for use by disabled patients.

Since the EEG patterns we can use are limited nowadays, we could adopt encoding methods to increase commands for controlling the robot. However, more commands would result in higher error rate. Thus, classification methods would be a core technology for improving CTU performance. Support vector machines or linear programming machines (LPMs) are potential tools for reducing the classification error rate. Moreover, in the field of electro-neurophysiology, researchers are prospecting for other controllable EEG patterns that may facilitate further development of BCI technology.

Furthermore, a robot agent should provide a subject with sufficient environmental information. However, excessive information (visual or sound) fed back by the robot will likely distract a subject, and may reduce BCI system accuracy. However, this issue of appropriate interface design, which is seldom addressed, is worthy of further investigation.

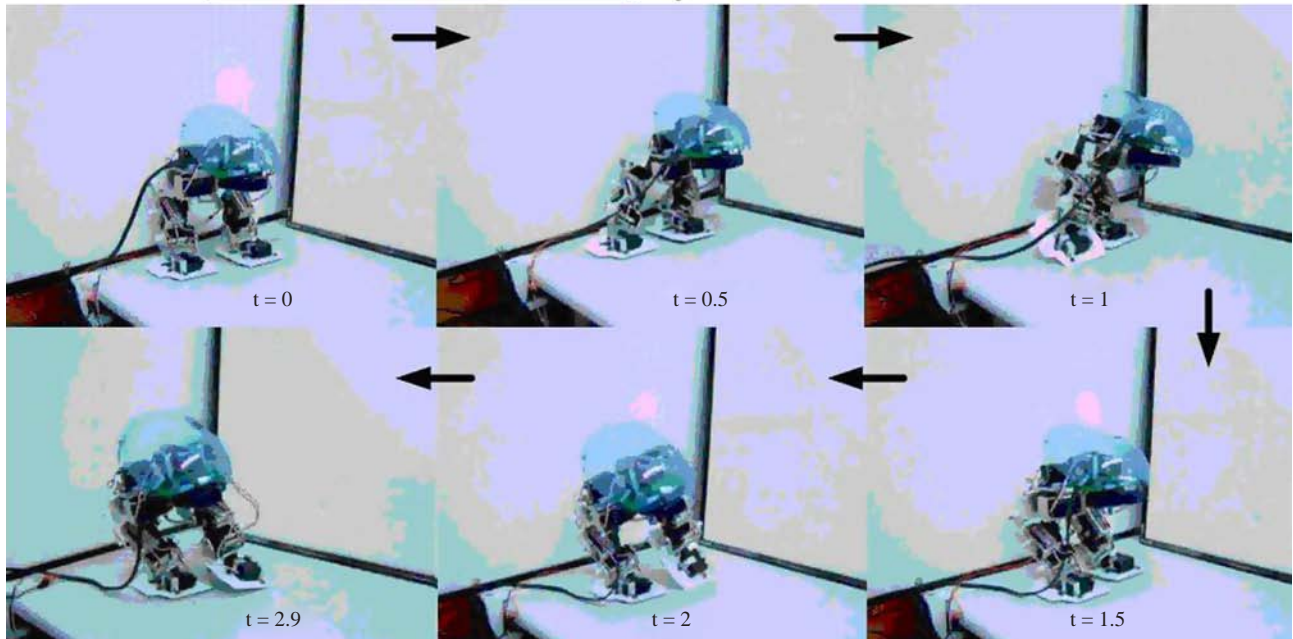
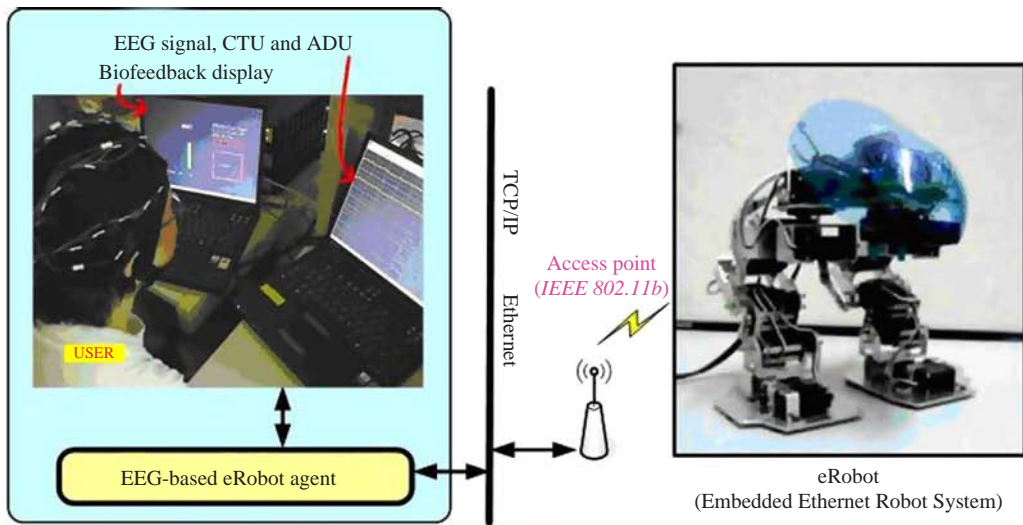
The eRobot architecture has also been utilized to develop a humanoid robot, “YamBall Man.” This novel architecture has a flexible and funny humanoid body, and because of the proposed EEG-based eRobot agent, it can perform various services. For instance, a patient could use the BCI system to control “YamBall Man” virtually, enabling it interact with a family. Additionally, if a user has health risks, the proposed robot agent can generate an alarm message and send it to hospital via e-mail, and issue a text message via a short message service (SMS) to a cell phone or PDA of a family member. Accordingly, this integration of BCI technology with the robot can support a novel home robot service. Figure 18 depicts this novel concept.

Figure 16 Combination of the CTU and the ADU



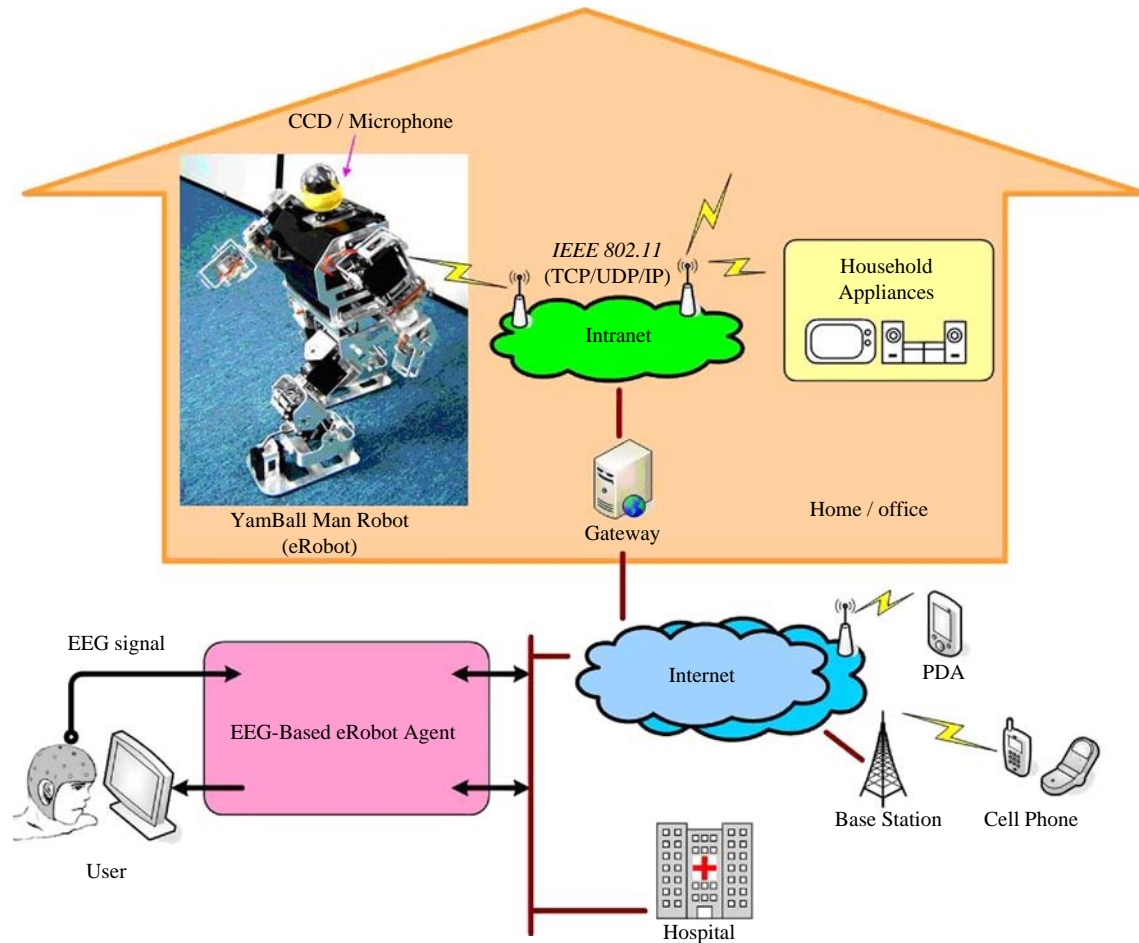
**Notes:** The left column presents the ADU results and the right column represents commands issued by the user. The top right of the screen displays a sequence of commands. An action will be determined according to the pre-defined R-L sequence

Figure 17 EEG-Based eRobot agent uses embedded TCP/UDP/IP technology and the BCI system



**Notes:** The eRobot is controlled only by the user's EEG. The user and the eRobot were separated (in different rooms). When an action command "go" was issued, the eRobot generated the walking trajectory of two leg gaits to make the biped robot move forward

**Figure 18** In the future, the EEG-based eRobot agent will utilize embedded TCP/UDP/IP technology integrated with the home network environment to provide more services for particular users



## References

- Bentham, J. (2002), *TCP/IP Lean: Web Servers for Embedded Systems*, 2nd ed., CMP Books, San Francisco, CA.
- Birch, G.E., Mason, S.G. and Borisoff, J.F. (2003), "Current trends in brain-computer interface research at the Neil Squire foundation", *IEEE Trans. Neural. Syst. Rehabil. Eng.*, Vol. 11 No. 2, pp. 123-6.
- Bishop, C.M. (1995), *Neural Networks for Pattern Recognition*, Clarendon, Oxford.
- Cheng, M., Gao, X., Gao, S. and Xu, D. (2001), "Design and implementation of a brain-computer interface with high transfer rates", *IEEE Trans. Biomed. Eng.*, Vol. 49, pp. 1181-6.
- Ganong, W.F. (1991), *Review of Medical Physiology*, Appleton & Lange, Connecticut, CT.
- Guger, C., Edlinger, G., Harkam, W., Niedermayer, I. and Pfurtscheller, G. (2003), "How many people are able to operate an EEG-based brain-computer interface (BCI)?", *IEEE Trans. Neural. Syst. Rehabil. Eng.*, Vol. 11 No. 2, pp. 145-7.
- Guger, C., Schlögl, A., Neuper, C., Walterspacher, D., Strein, T. and Pfurtscheller, G. (2001), "Rapid prototyping of an EEG-based brain-computer interface (BCI)", *IEEE Trans. Neural. Syst. Rehabil. Eng.*, Vol. 9, pp. 49-58.
- Hwang, B-H., Kong, J-S., Lee, B-H., Kim, J.-G. and Huh, U-Y. (2005), "ZMP compensation algorithm for stable posture of a humanoid", *Proceedings of International Conference on Computer Applications in Shipbuilding*, CDROM, KINTEX, Gyeonggi-Do, UP12-09.
- Karim, A.A., Hinterberger, T., Richter, J., Mellinger, J., Neumann, N., Flor, H., Kübler, A. and Birbaumer, N. (2006), "Neural internet: web surfing with brain potentials for the completely paralyzed", *Neurorehabil Neural Repair*, Vol. 20 No. 4, pp. 508-15.
- Klimesch, W. (1996), "Memory processes, brain oscillations and EEG synchronization", *Int. J. Psychophysiol.*, Vol. 24, pp. 61-100.
- Kostov, A. and Polak, M. (2000), "Parallel man-machine training in development of EEG-based cursor control", *IEEE Trans. Rehabil. Eng.*, Vol. 8, pp. 203-5.
- Liao, H.-C. and Lo, P.-C. (2006), "Meditation EEG overview based on subband features quantified by AR model", *J. Intl. Soc. Life. Info. Sci.*, Vol. 24 No. 1, pp. 119-28.
- Middendorf, M., McMillan, G., Calhoun, G. and Jones, K.S. (2000), "Brain-computer interfaces based on the steady-state visual-evoked response", *IEEE Trans. Rehabil. Eng.*, Vol. 8, pp. 211-4.



- Oppenheim, A.V., Schaffer, R.W. and Buck, J.R. (1998), *Discrete-Time Signal Processing*, Prentice-Hall, Upper Saddle River, NJ.
- Pfurtscheller, G. and Neuper, C. (2001), "Motor imagery and direct brain-computer communication", *IEEE Proc.*, Vol. 89, pp. 1123-34.
- Pfurtscheller, G., Neuper, C., Guger, C., Harkam, W., Ramoser, H., Schögl, A., Obermaier, B. and Pregenzer, M. (2000), "Current trends in graz brain-computer interface (BCI) research", *IEEE Trans. Rehabil. Eng.*, Vol. 8, pp. 216-9.
- Pfurtscheller, G., Neuper, C., Müller, G.R., Obermaier, B., Krausz, G., Schögl, A., Scherer, R., Graimann, B., Keinrath, C., Skliris, D., Wortz, M., Supp, G. and Schrank, C. (2003), "Graz-BCI: state of the art and clinical applications", *IEEE Trans. Neural. Syst. Rehabil. Eng.*, Vol. 11 No. 2, pp. 177-80.
- Pineda, J.A., Silverman, D.S., Vankov, A. and Hestenes, J. (2003), "Learning to control brain rhythms: making a brain-computer interface possible", *IEEE Trans. Neural. Syst. Rehabil. Eng.*, Vol. 11 No. 2, pp. 181-4.
- Smith, R. (1998), "Intelligent motion control with an artificial cerebellum", PhD thesis, Dept of Electrical and Electronic Engineering, University of Auckland, Auckland.
- Vidal, J. (1973), "Toward direct brain-computer communication", *Annu. Rev. Biophys. Bioeng.*, pp. 157-80.

- Wolpaw, J.R. and McFarland, D.J. (2004), "Control of a two-dimensional movement signal by a noninvasive brain-computer interface in humans", *PNAS*, Vol. 101 No. 51, pp. 17849-54.
- Wolpaw, J.R., Birbaumer, N., Heetderks, W.J., McFarland, D.J., Peckham, P.H., Schalk, G., Donchin, E., Quatrano, L.A., Robinson, C.J. and Vaughan, T.M. (2000), "Brain-computer interface technology: a review of the first international meeting", *IEEE Trans. Rehabil. Eng.*, Vol. 8, pp. 164-73.
- Wu, L-W. and Hu, J-S. (2004), "Robot control system using embedded network", Taiwan Patent, Invention No. I238622.
- Wu, L-W. and Hu, J-S. (2005), "Distributed embedded real-time ethernet platform for robots control", *Proceeding of IEEE International Conference on Mechatronics*, pp. 10-12.

### Further reading

- Lightner Engineering (2000), "PicoWeb™", available at: [www.picoweb.net](http://www.picoweb.net)

### Corresponding author

Li-Wei Wu can be contacted at: [liwel.ece89g@nctu.edu.tw](mailto:liwel.ece89g@nctu.edu.tw)